SUPPORTING INFORMATION

X-ray Photoelectron Spectroscopy.

Figure S1 shows high resolution X-ray photoelectron spectroscopy of carbon 1s region acquired for MHA (red) and HDT (green). The principal peak at 284.7 eV is characteristic for aliphatic hydrocarbons. The high binding energy peak in the MHA spectrum at 289.3 eV arises from the bond between an α-carbon and a carbonyl group. Our data are in excellent agreement with published work by Bain *et al.*[12].

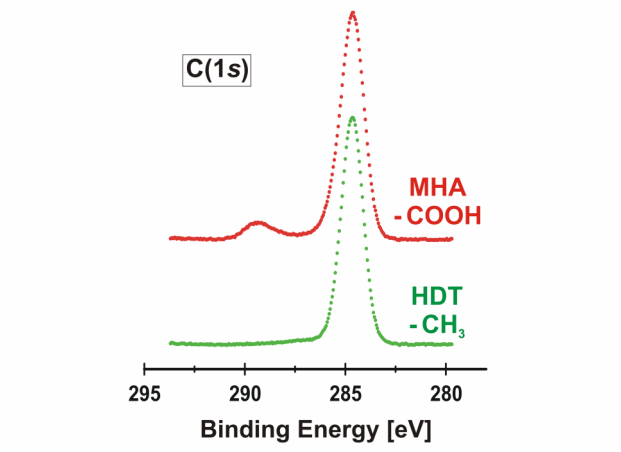

Figure S1: *XPS carbon 1s spectra of MHA and HDT SAMs.*

Evaluation Software and ANOVA Model.

The bending signals obtained from a cantilever array experiment are typically associated with multiple parameters such as separate cantilever arrays, an individual cantilever within the array, number of repeated measurements, and, in case of the pH experiments as presented herein, deprotonation or protonation reactions. The development of an appropriate evaluation algorithm by means of custom written software was found to be essential for a rapid analysis of large data sets with minimal user bias. Furthermore, a statistical model for an analysis of variance (ANOVA) was developed to estimate and to decompose the overall variability resulting from multiple

measurements into different components. The software used to evaluate the raw signals was written in IDL 6.0 (ITT Visual Information Solutions Co., Boulder, CO, U.S.A.), while the ANOVA was carried out using the statistical software package Minitab 13.32 (Minitab Inc., State College, PA, U.S.A.).

Consider the experiment performed in a single cycle of pH 4.5 / 6.0 / 4.5 sodium phosphate solutions at constant ionic strength of μ = 0.1. This experiment involved a total of 19 cantilevers distributed on four separate cantilever arrays and coated with either HDT or MHA SAM. Two measurements were made on each cantilever, first the deprotonation absolute stress on switching from pH 4.5 to pH 6.0 and then the protonation absolute stress on switching back to pH 4.5. It should be noted that the following criteria were applied to discard an individual cantilever from the evaluation: (a) broken or visibly damaged cantilevers and (b) cantilevers which failed the heating test performed to align the SLD with the cantilever array. Both criteria were applied consistently throughout the data presented in this paper.

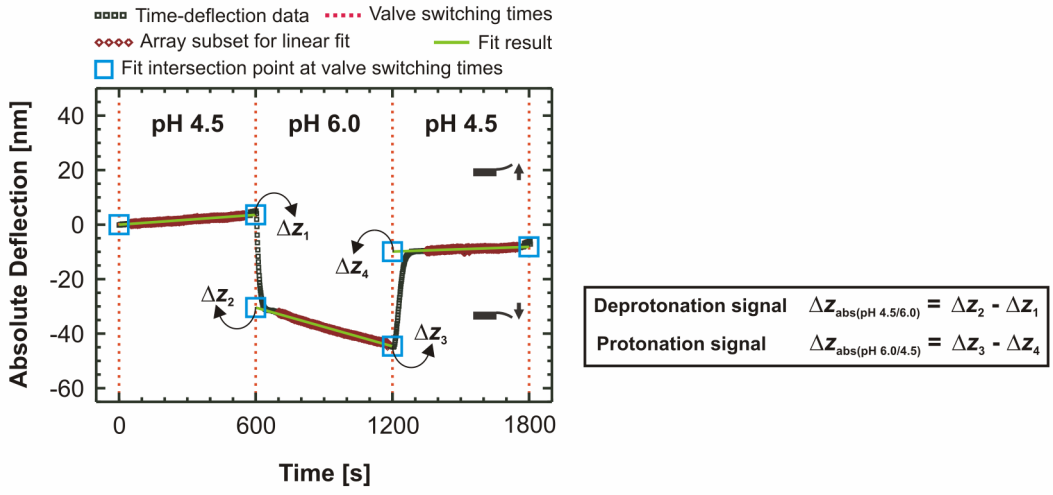

Figure S2: *Semi-automated analysis of surface stress measurements.*

The principle of the raw data evaluation algorithm is demonstrated in Figure S2 using an absolute signal (hollow black squares) acquired by switching from pH 4.5 / 6.0 / 4.5 sodium phosphate

solutions. A linear fit was applied to the raw time-deflection data points generated in each particular liquid environment. Subsequently, the fitted curves were extrapolated (green solid lines) to the onsets of liquid exchange (light blue hollow squares) to calculate the following two bending signals: (1) the *deprotonation* signal $\Delta z_{\text{abs (pH4.5/6.0)}}$ triggered by pH switch from 4.5 to 6.0 (2) and the *protonation* signal $\Delta z_{\text{abs (pH6.0/4.5)}}$ triggered by pH switch from 6.0 back to 4.5. In both cases the bending signal (the vertical difference between the blue squares in Figure S2) was calculated by subtracting the intersection value of the fitted curve obtained at pH 6.0 from the intersection value of the fitted curve obtained at pH 4.5. The resulting bending signals obtained from the IDL software were converted to measures of absolute stress using Stoney's equation (Equation 1), with L = 450 μm, giving $\Delta\sigma_{\text{abs}} = 0.24067\ \Delta z_{\text{abs}}$. Please note that more significant figures have been used in the calculations than are shown in Tables S2 and S3 presented later in this section. This method of measuring the stresses has two consequences. Firstly the contrast between deprotonation and protonation will be confounded with any order effect, since deprotonation is always measured first. Secondly the within-cantilever measurement errors, e_{sti1} and e_{sti2}, defined below, could be correlated (allowance is made for this in the analysis).

The ANOVA was based upon a linear model, (Equation S1), which describes how the absolute stress, hereafter termed *y*, depends on the various fixed and random factors. A general introduction to the ANOVA is given in standard text books[20]. Let y_{stik} be the *k*th observation on the *i*th cantilever in the (*st*)th cell (Array *s* and SAM *t*), then:

$$y_{stik} = M + A_s + T_t + (AT)_{st} + u_{sti} + P_k + (AP)_{sk} + (TP)_{tk} + (ATP)_{stk} + e_{stik} \qquad \text{(Equation S1)}$$

with k = 1, 2; i = 1, ... n_{st} ; t = 1, 2; s = 1, 2, 3, 4; where appropriate constraints are put on the fixed parameters (to remove redundancy). The random errors, u_{sti} and e_{stik}, are assumed to be normally

distributed with variances σ_u^2 and σ_e^2, respectively. The correlation between e_{sti1} and e_{sti2} is ρ, but otherwise all *u*'s and *e*'s are assumed to be independent. The within-cantilever random error, e_{stik}, models the unexplained or residual variation for a single cantilever, while the between-cantilever error, u_{sti}, accounts for the extra differences between cantilevers (in the same array and with the same SAM) over and above that which would arise from the within-cantilever variation. The parameters A_s, T_t, P_k represent the main effects of the three fixed factors, cantilever array, SAM, and deprotonation/protonation, respectively. The remaining parameters are the two and three term interactions of these three factors. The number, n_{st}, of cantilevers in each Array by SAM cell are given in Table S1. Ideally, and by our design, each cantilever array would contain the same number (four) of cantilevers coated with MHA as with HDT, however, as explained earlier some cantilevers could not be used.

Table S1: Number n_{st} of cantilevers in each array by SAM cell.

	Array (*s*)				
SAM (*t*)	1	2	3	4	**Totals** $\sum_s n_{st}$
1 (HDT)	3	2	2	2	9
2 (MHA)	3	2	2	3	10
Totals $\sum_t n_{st}$	6	4	4	5	19

Table S2 gives the absolute stresses for these 19 cantilevers, the means and the differences for the deprotonation and protonation pairs, and the Array by SAM cell means. On examination Array 3 appears atypical. For our purpose, which is to gain understanding of the processes, it is important to retain atypical results, although, before the technology is ready to be used diagnostically, some further inclusion/exclusion protocols may need to be developed.

Table S2: Table of data, means, and differences. *SAM: $t = 1$ for HDT, $t = 2$ for MHA.

Array (s)	SAM* (t)	Cantilever $i(st)$	Deprotonation [mN/m] (y_{sti1})	Protonation [mN/m] (y_{sti2})	Mean [mN/m] $1/2(y_{sti1} + y_{sti2})$	Difference [mN/m] $(y_{sti1} - y_{sti2})$	
1	1	1	-8.50	-8.40	-8.45	-0.10	
1	1	2	-9.51	-9.24	-9.37	-0.26	
1	1	3	-8.52	-8.23	-8.38	-0.29	
1	1	Mean	-8.84	-8.62	-8.73	-0.22	
1	2	1	-7.70	-7.51	-7.61	-0.19	
1	2	2	-7.89	-7.58	-7.74	-0.31	
1	2	3	-7.63	-7.48	-7.56	-0.14	
1	2	Mean	-7.74	-7.52	-7.64	-0.21	
2	1	1	-7.73	-7.32	-7.52	-0.41	
2	1	2	-6.93	-6.74	-6.84	-0.19	
2	1	Mean	-7.33	-7.03	-7.18	-0.30	
2	2	1	-6.28	-5.68	-5.98	-0.60	
2	2	2	-6.76	-6.45	-6.61	-0.31	
2	2	Mean	-6.52	-6.06	-6.29	-0.46	
3	1	1	-1.42	-1.83	-1.62	0.41	
3	1	2	-0.96	-1.44	-1.20	0.48	
3	1	Mean	-1.19	-1.64	-1.41	0.45	
3	2	1	1.54	1.37	1.46	0.17	
3	2	2	0.00	-0.34	-0.17	0.34	
3	2	Mean	0.77	0.52	0.64	0.25	
4	1	1	-5.17	-5.22	-5.20	0.05	
4	1	2	-5.44	-5.49	-5.46	0.05	
4	1	Mean	-5.31	-5.35	-5.33	0.05	
4	2	1	-5.13	-4.86	-4.99	-0.26	
4	2	2	-4.21	-3.87	-4.04	-0.34	
4	2	3	-4.19	-4.00	-4.09	-0.19	**Grand Mean**
4	2	Mean	-4.51	-4.24	-4.38	-0.26	**-5.34 mN/m**

The ANOVA partitions the Corrected Total Sum of Squares $\sum_s \sum_t \sum_i \sum_k \left(y_{stik} - \bar{y}_{....}\right)^2 = 335.26$ according to the individual Sources of Variability, where $\bar{y}_{....} = (1/38) \sum_s \sum_t \sum_i \sum_k y_{stik} = -5.34$ mN/m. The resultant ANOVA table is shown in Table S3. Each of rows 2 to 10 in Table S3 corresponds to a factor, an interaction or a random term in the model (Equation S1).

Table S3: ANOVA for the cantilever array data.

	1	2	3	4	5	6	7
1	**Sources of Variability**	**DF***	**Sequential Sum of Squares [(mN/m)^2]**	**Adjusted Sum of Squares [(mN/m)^2]**	**Sequential Mean Square [(mN/m)^2]**	***F*-value**	***p*-value**
2	Array	3	312.368	311.229	104.123	185.58	< 0.0005
3	SAM	1	14.003	14.263	14.003	24.96	< 0.0005
4	Array × SAM	3	1.841	1.841	0.614	1.09	0.392
5	Between-Cantilever Error	11	6.172	6.172	0.561	95.34	< 0.0005
6	Deprotonation/Protonation	1	0.118	0.072	0.118	20.06	0.001
7	Array × Deprotonation/Protonation	3	0.602	0.600	0.201	34.12	< 0.0005
8	SAM × Deprotonation/Protonation	1	0.056	0.063	0.056	9.49	0.010
9	Array × SAM × Deprotonation/Protonation	3	0.034	0.034	0.011	1.91	0.187
10	Within-Cantilever Error	11	0.065	0.065	0.006		
11	Corrected Total	37	335.259				

* **DF: Degrees of freedom.**

The Sequential Sum of Squares given in column 3 of Table S3 corresponds to the decrease in the residual sum of squares when a new term is added to the model containing all those terms added prior to this new term (terms were added in the order shown in the table). Conversely, the Adjusted Sum of Squares given in column 4 corresponds to the decrease in the residual sum of squares when a new term enters a model which already contains all the other terms. Here we use the sequential sum of squares as we are primarily interested in the effects which arose from the difference in the SAM cantilever coating. However, the use of the adjusted sum of squares was found not to alter the qualitative results of the ANOVA. The Sequential Mean Squares given in column 5 of Table S3 were obtained by dividing a sequential sum of squares by its Degrees of Freedom, given in column 2 of Table S3. The *F*-value given in column 6 of Table S3 is the mean square ratio, *i.e.*, the mean square for a particular source of variability divided by the mean square for its associated random error term. The *p*-value in column 7 of Table S3 is the probability of obtaining such a large *F*-value if the true value of the relevant parameters were zero. A small *p*-value is interpreted as evidence that the relevant parameters are not zero.

The Within-Cantilever Error mean square in row 10 estimates the *effective* within-cantilever error variance, $\sigma_e^2\,(1-\rho)$, and Between-Cantilever Error mean square in row 5 estimates the *total* between-cantilever error variance, $\sigma_e^2\,(1+\rho)\,+\,2\sigma_u^2$. From the *F*- and *p*-values in row 5 there is clear evidence that the *total* between-cantilever error variance is greater than the *effective* within-cantilever error variance, however, we cannot determine how much this is due to σ_u^2 rather than to ρ. Fortunately, the interpretation of the rest of the ANOVA table is not affected. Deprotonation/Protonation and its interactions with Array and SAM in the lower half of Table S3 involve only within-cantilever variation as the deprotonation and protonation reactions were observed on the same cantilever, so the appropriate random variation term is the mean square 0.006 in row 10. This allows quite small main effects and interactions to be detected (rows 6, 7, and 8).

There is evidence that the magnitude of the absolute deprotonation stress tends to be slightly more negative (compressive) than the absolute protonation stress, and that the size of this difference varies between SAMs (greater for MHA than for HDT) and between cantilever arrays. Array, SAM, and Array by SAM in the upper half of Table S3, involve the total between-cantilever error variance, so the appropriate denominator mean square is 0.562 in row 5. From the *F*- and *p*-values in rows 2, 3, and 4, we conclude that there is clear evidence of differences between cantilever arrays and between SAMs but no evidence of an interaction. This is important as it suggests that the differential stress will not change from one cantilever array to another. To estimate the differential stress between MHA and HDT we used $(1/4)\sum_s (\bar{y}_{s2\cdot\cdot} - \bar{y}_{s1\cdot\cdot}) = 1.24$ mN/m. This has standard error $\sqrt{(7/64)(\sigma_e^2(1+\rho) + 2\sigma_u^2)}$, where $\bar{y}_{st\cdot\cdot} = (1/2n_{st})\sum_i \sum_k y_{stik}$ is the (*st*)th cell mean. Using the mean square in row 5 to estimate $(\sigma_e^2(1+\rho) + 2\sigma_u^2)$ gives an estimated standard error of 0.24 mN/m. Finally, it is useful to estimate the change in differential stress between protonation and deprotonation. We averaged the estimates for each array, giving $(1/4)\sum_s ((\bar{y}_{s2\cdot2} - \bar{y}_{s1\cdot2}) - (\bar{y}_{s2\cdot1} - \bar{y}_{s1\cdot1})) = 0.18$ mN/m with standard error $\sqrt{(7/16)\sigma_e^2(1-\rho)}$. When the residual error mean square (row 10) is substituted for $\sigma_e^2(1-\rho)$, this gives an estimated standard error of 0.05 mN/m. Thus the study has shown that from the 38 observations for pH 6.0 and using sodium phosphate solutions we were able to estimate the differential stress with a relative standard error of about 20 per cent. Under these conditions the differential stress was tensile. The measurement of differential stress made during protonation was slightly more positive (tensile) than during deprotonation, the difference being measured in our experiment with a relative standard error of about 30 per cent.

Future experiments to investigate the kinetics of surface stress evolution will include investigation of the use of non-linear functions to fit the raw data and further study of the nature and chemical

implications of different sources of variation, including the within- and between-cantilever effects of successive cycles and measurement order[21].